HORIZON EUROPE PROGRAMME

TOPIC HORIZON-CL5-2021-D3-03-03

GA No. 101083700

HYBRID TANDEM CATALYTIC CONVERSION PROCESS TOWARDS HIGHER OXYGENATE EFUELS

E-TANDEM - Deliverable Report

Deliverable 3.3 – Fuel-Components Interaction

Funded by the European Union

Deliverable No.	E-TANDEM D3.3	
Related WP	WP3	
Deliverable Title	Fuel-components interaction	
Deliverable Date	2025-04-30	
Deliverable Type	REPORT	
Dissemination level	Public (PU)	
Author(s)	Werner Willems (T4F), Frans Kremer (OWI)	2025-10-15
Checked by	Karin Engeländer (OWI)	2025-10-29
Reviewed by (if applicable)		
Approved by	Gonzalo Prieto (CSIC) – Project coordinator	2025-10-31
Status	Final	2025-11-05

Project summary

E-TANDEM's ambition is to unlock an efficient and direct production of a new higher-oxygenate diesel-like e-fuel for the marine and heavy-duty transport sectors. This oxygenated fuel is directly produced from water, CO_2, as the sole carbon source, and renewable power as the sole energy input, in a once-through hybrid catalytic conversion process integrating three major catalysis branches: (1) high-pressure electrocatalysis *syngas* production coupled to a tandem catalytic e-syngas conversion, encompassing (2) thermocatalysis with solid catalysts and (3) chemocatalysis with molecular complexes. The project will demonstrate the new e-fuel production process at bench-scale and assess its capacity to cope with fluctuating energy inputs.

Executive summary

Carbon-neutral, high-energy density e-fuels are critical to de-fossilize the legacy fleet for all ICE-based applications and are in particular mandatory for long-haul, heavy-duty road, marine, and aviation transport, where high energy density solutions are required. The introduction of e-fuels for rapid market penetration faces several challenges. Apart from the higher cost of these products, additional challenges arise from the compatibility of existing and new applications, which have been designed on the assumption that existing standards will be met even if the source of the energy carrier is sustainable, which is generally not the case. Ideally, these new fuels could be blended with existing fuels, allowing a transition from fossil fuel to a sustainable product in the future.

The E-TANDEM project develops and validates, at bench scale, the first direct process for the selective production of carbon-neutral higher oxygenate e-fuels (HOEF) as a replacement for fossil diesel. The focus is on heavy-duty, hard to abate transport sectors, particularly waterborne transport, but also heavy-duty road transport. This mildly oxygenated fuel is composed of higher (C_{5+}), aliphatic alcohols and their derivative aliphatic ethers, and it is directly produced from CO_2 as the sole carbon source, and renewable power as the sole energy input, in a once-through hybrid catalytic conversion process integrating three major catalysis branches: electrocatalysis syngas production, coupled to a tandem catalytic e-syngas conversion encompassing thermocatalysis with solid catalysts and chemocatalysis with molecular complex catalysts. The project demonstrates the new e-fuel production process at bench-scale and assesses its capacity to cope with fluctuating energy inputs.

This deliverable report D3.3 emerges from R&D activities performed in work-package (WP) 3. It summarizes the results from studies of the fuel-components interaction properties of surrogate fuels mixtures in HOEF realizations, i.e. (i) a mixture of higher (C_4-C_9) alcohols and (ii) a mixture of higher (C_8-C_{18}) ethers, which have been developed in WP2 from commercially available neat alcohol compounds, while closely simulating compositions obtained through the tandem catalysis e-fuel production concept developed in the project. Emphasis is placed on the blending behaviour of the HOEF with state-of-the-art marine gas oil (MGO), to ascertain the drop-in potential of the new e-fuel compositions. Fuel-components characteristics of the HOEF blends with MGO are determined and discussed with the aim to identify compliance or deviations with the state-of-the art engine materials in shipping industry.

Contents

1 Introduction 8
2 Methods 9
2.1 Background 9
2.2 Procedures 10
2.3 Data Analysis 15
2.4 Overview on fuels and materials tested 15
3 Results & Discussion 18
3.1 Compatibility immersion test 18
3.2 Rapid aging test 25
3.3 Hardware-in-the-loop test 30
3.4 Contribution to project (linked) Objectives 32
3.5 Contribution to major project exploitable result 32
4 Conclusion and Recommendation 33
5 Risks and interconnections 34
5.1 Risks/problems encountered 34
5.2 Interconnections with other deliverables 34
6 Deviations from Annex 1 35
7 References 36
8 Acknowledgement 37

List of Figures

Figure 2-1 Teflon cylinder and specimen holder dimensions..... 11
Figure 2-2 Overview of BigOxi reactors and preparation of the different sample materials inside the reactors..... 12
Figure 2-3 P&ID of the HIL test bench 13
Figure 2-4 Typical Test-Setup for DIN 54505 Testing of stretch testing of rubber and polymers 15
Figure 3-1 Overview of immersion test containers at start 19
Figure 3-2 Deposits on container bottom during monthly inspection, container 1, 6 and 14..... 19
Figure 3-3 42CrMo4 with increasing immersion time in 10% (left) and 20% (right) ether surrogate (left fuel-immersed, right vapor-exposed section). 20
Figure 3-4 W-FA-55SiCr-QT-SP with increasing immersion time in 10% (left) and 20% (right) ether surrogate (left fuel-immersed, right vapor-exposed section). 21
Figure 3-5 HS6-5-2 with increasing immersion time in 10% (left) and 20% (right) ether surrogate (left fuel-immersed, right vapor-exposed section). 21
Figure 3-6 18CrNiMo7-6 with increasing immersion time in 10% (left) and 20% (right) ether surrogate (left fuel-immersed, right vapor-exposed section). 22
Figure 3-7 FVMQ (left) and FKM (right) with increasing immersion time in 20% ether surrogate (left fuel-immersed, right vapor-exposed section). 23
Figure 3-8 FVMQ and FKM relative weight change with increasing immersion time in 10% (left) and 20% (right) ether surrogate. 23
Figure 3-9 FVMQ and FKM silicon release into the fuel over the test period of 6 months. 25
Figure 3-10 Results of the Tensile Streng Tests for FVMQ and FKM after 6 months aging 25
Figure 3-11 W-FA-55SiCr-QT-SP before (left) and after (right) BigOxi testing in 20% ether surrogate (left fuel-immersed, right vapor-exposed section). 26
Figure 3-12 42CrMo4 before (left) and after (right) BigOxi testing in 20% ether surrogate (left fuel-immersed, right vapor-exposed section). 27
Figure 3-13 18CrNiMo7-6 before (left) and after (right) BigOxi testing in 20% ether surrogate(left fuel-immersed, right vapor-exposed section). 27
Figure 3-14 HS6-5-2 before (left) and after (right) BigOxi testing in 20% ether surrogate (left fuel-immersed, right vapor-exposed section). 27
Figure 3-15 FKM before (left) and after (right) BigOxi testing in 20% ether surrogate (left fuel-immersed, right vapor-exposed section). 27
Figure 3-16 FVMQ before (left) and after (right) BigOxi testing in 20% ether surrogate (left fuel-immersed, right vapor-exposed section). 27
Figure 3-17 42CrMo4 before (left) and after (right) BigOxi testing in 50% ether surrogate (left fuel-immersed, right vapor-exposed section). 27
Figure 3-18 18CrNiMo7-6 before (left) and after (right) BigOxi testing in 50% ether surrogate (left fuel-immersed, right vapor-exposed section). 27
Figure 3-19 FKM before (left) and after (right) BigOxi testing in 50% ether surrogate (left fuel-immersed, right vapor-exposed section). 27
Figure 3-20 FVMQ before (left) and after (right) BigOxi testing in 50% ether surrogate (left fuel-immersed, right vapor-exposed section). 28
Figure 3-21 FVMQ and FKM relative weight change. 28

Figure 3-22 Results of the Tensile Streng Tests for FVMQ and FKM after rapid aging 29
Figure 3-23 Hardware in the Loop-Testbench used for the injection system evaluation for the different blends 30
Figure 3-24 Common-rail injector and injector nozzle used for the HiL-tests 30
Figure 3-25 Comparison of HiL performance for degradated MGO and high quality MGO 31

List of Tables

Table 2.1 Overview of the blends availability for testing. 16
Table 2.2 Overview of the fuel volumes required per type of analysis test. 16
Table 2.3 Overview of the materials and their chemical composition for the corrosion test. 17
Table 3.1 Overview of the materials and their exposed fuel composition for the corrosion test. . 18
Table 3.2 Overview of the materials and their exposed fuel composition for the rapid aging test. 26
Table 3.3 Overview of the Si leaching for the polymer materials after the rapid aging test. 29

Abbreviations & Definitions

Abbreviation	Explanation
FKM	Fluorkautschukmaterial (fluoroelastomer material, aka fluorocarbon rubber)
FVMQ	Fluor Vinyl Methyl Silicone rubber
HIL	Hardware-In-the-Loop
HOEF	Higher-oxygenate e-Fuel
ICP-OES	Inductively coupled plasma optimal emission spectroscopy
MGO	Marine Gas Oil

Item	Definition
DMA	Marine Gas Oil grade. Marine Gas Oil with low sulphur content, distilled and high Quality
DMB	Marine Gas Oil grade. Marine Gas Oil with more remnants as DMA
DMX	Marien Gas Oil grade. Often referred to as a special light distillate, DMX is designed for high-speed engines that require fuels with lower viscosity and density.
DMX	Marine Gas Oil grade. The heaviest among the distillates, DMZ is used primarily for emergency engines and some types of medium-speed engines

1 Introduction

This report relates to Work Package 3 (WP3) within the E-TANDEM project. WP3 deals with the characterization of the higher oxygenate e-fuels (HOEF), the analysis of their blending behaviour with base, state-of-the-art fuels, as well as the study of system compatibility aspects of HOEF and its blends.

The research summarized in this report thus covers the need to provide an early assessment of the ignition behaviour of the herein proposed HOEF e-fuel, regarding its use as a diesel replacement in applications of marine and heavy-duty transport, as well as to assess the effects of its mildly oxygenated character on the tailpipe emission profile.

Specific goals set for WP3 are:

1. To physico-chemically characterize the higher oxygenate HOEF e-fuel in its two realizations, i.e. mixture of higher aliphatic alcohols (with hydrocarbons) or mixture of higher ethers and study its blending behaviour with baseline fuels.

2. To evaluate the ignition behaviour and soot formation characteristics of selected HOEF e-fuel formulae.

3. To assess the fuel-system compatibility for HOEF and its blends: interaction with materials, lubricants, etc., in current-fleet systems.

Specifically, this deliverable report D3.3 addresses the last goal, while the goals 1 and 2 are reported in reports D3.1 and D3.2, respectively.

The present report is organized as follows. Chapter 2 describes the considerations and method-selection, as well as the experimental methodology applied for fuel-component interaction. In Chapter 3 the experimental results are provided and discussed. Finally, in Chapter 4, conclusions and recommendations are given.

2 Methods

This chapter outlines the considerations, and the selected experimental methodologies used for the fuel-components characterization of HOEF e-fuel. Section 2.1 provides background considerations, while section 2.2 describes the procedures and their particulars in this project. Where applicable, further data analyses are given in section 2.3.

2.1 Background

Within the planned project timeline, the final e-fuel from the production process will only become available near the end of the project and at volumes which are insufficient to perform some of the fuel characterization tests and blending analyses which are of concern in this report. Therefore, so-called e-fuel surrogates have been produced in the context of the project's WP2, and provided for activities in WP3, early in the project. The background and production details on the surrogate HOEF in a multi-liter scale have been detailed in Deliverable report D2.1.

Two mixtures of known composition have been produced, as surrogates for two different realizations of the HOEF e-fuel:

(i) A first mixture, hereafter referred to as "alcohol surrogate", which consists of a mixture of linear and branched alcohols in the carbon chain-length range of C_4-C_9; and

(ii) A second mixture, hereafter referred to as "ether surrogate", which consists of a mixture of C_8-C_{18} ether derivatives and which has been obtained via catalytic dehydration of the alcohol mixture in the "alcohol surrogate".

These mixtures have been produced from commercially available alcohol compounds in neat form. In the first case just by blending; in the second instance via catalytic dehydration of higher alcohols to higher ethers. Moreover, the composition of the "alcohol surrogate" mixture has been designed to mimic closely that obtained in lab-scale tests of the e-fuel production process developed in E-TANDEM, both in terms of alcohol chain-length distribution as well as in terms of the molar ratio of linear (*n*) to branched (*iso, 2-methylated*) alcohols at each specific chain length.

With the objective of assessing the potential of these e-fuel compositions to be blended with existing fuels, as well as to comply (in neat or blended forms) with existing fuel regulations, which is a critical aspect for a fast adoption the following two methods have been considered as relevant:

(i) Laboratory long duration and accelerated material compatibility tests [1]; and

(ii) Hardware-in-the loop tests [2].

This approach enables early feedback on the e-fuel properties and provides an effective means for potentially guiding the optimization of the production process for the final e-fuel product.

2.2 Procedures

2.2.1 Laboratory immersion test

The primary objective of the compatibility test is to evaluate the influence of fuel on the corrosion behavior of metallic materials and on the seal materials. Conventionally, the assessment of corrosion behavior has been facilitated by the implementation of two primary methodologies: the copper corrosion test (DIN EN ISO 2160) [3] and the steel corrosion test (ASTM D665-06) [4]. The HOEF e-fuels have already been evaluated using the copper corrosion test, and the results indicated minimal corrosion effects (see deliverable D3.1). However, the steel corrosion test, which necessitates testing at 60°C in an open apparatus, is not applicable to volatile diesel-like fuels due to safety concerns and the possibility of evaporation. To address this limitation, a method was employed in this study, where specimen rods made from various materials were exposed to the test fuels in sealed containers.

The objective of compatibility studies is to ascertain the manner in which fuels interact with materials such as metals, plastics, and elastomers. This research endeavour is undertaken to identify potential effects, including but not limited to swelling, corrosion, and surface changes. This is of paramount importance not only for the prevention of material failure but also for the maintenance of long-term safety and engine performance. The VDA 230-207 standard [1] delineates a methodology for the evaluation of the corrosion behavior of materials (primarily metals) when exposed to fuel or liquid chemicals under simulated conditions. Laboratory-based immersion tests are performed using both standard metal samples and real automotive parts. For diesel fuels, sealed glass containers are utilized. Test materials are exposed to both the liquid and vapor phases of fuels. In order to circumvent cross-reactions, each container is tested with a single material type. The fuel and materials are exposed to elevated temperatures to expedite the aging process; however, the application of heat is meticulously regulated to prevent the fuel from undergoing decomposition or becoming unstable. The containers are stored for an extended period to observe whether corrosion occurs.
To avert photo-induced degradation or reactions, the glass containers are enveloped in aluminum foil throughout the duration of the exposure period. The sealed container is subsequently stored at 60°C within a climate-controlled chamber. On a weekly basis, a visual inspection of the contents is conducted to ascertain the presence of any alterations, including discoloration, sediment formation, or the accumulation of corrosion deposits. At four-week intervals, the specimen rod is extracted, thoroughly rinsed with ethanol, and dried. Subsequently, the rod is weighted and photographed. Then, the test fuel is replaced, and the clean rod is placed in fresh fuel for continued exposure. The utilized blend is maintained for the purpose of ICP-OES analysis, which is employed to quantify metal leaching (see section 2.2.4).

According to the VDA 230-207 standard [1], the recommended minimum ratio between the volume of test liquid and the surface area of the specimen is 1.3 cubic centimeters of liquid per 1.0 square centimeter of wetted surface area. In this method, each metallic specimen rod is precisely measured at 10 cm in length and 8 mm in diameter, with a maximum surface roughness of 3.2 µm.
In order to comply with the standard for the available glass container, the test setup for a rod includes a Teflon cylinder with a length of 70 millimeters, an outer diameter of 50 millimeters, and an internal diameter of 31 millimeters. This cylinder is placed in the container along with the specimen rod (see

Figure 2.1). The apparatus is designed to include a Teflon holder, which is intended to securely position the two rods per container during testing. This configuration is intended to prevent contact between the rod and the glass wall. The container is filled with 50 milliliters of test fuel. For a specific material (W-FA-55SiCr-QT-SP, exclusively available in a spring configuration), a comparable seal container is employed, though with 100 milliliters of test fuel and the absence of Teflon components. This is due to the fact that the configuration in question has already been demonstrated to meet the minimum volume-to-surface area ratio stipulated by the aforementioned standard. In this instance, a single spring specimen is subjected to testing, with half of the specimen submerged in the fuel.

In addition to metal samples, elastomers were incorporated into the compatibility test to assess their potential interaction with the test fuel. Although no corrosion effects are anticipated due to their non-metallic nature, the objective of the study is to evaluate chemical compatibility, particularly with regard to mass loss, swelling, or degradation of the rubber materials. For the specimens in question, a similar seal container is employed, containing 100 milliliters of test fuel and a Teflon cylinder devoid of a Teflon holder. Tensile testing was performed on the polymer specimens (see Section 2.2.5).

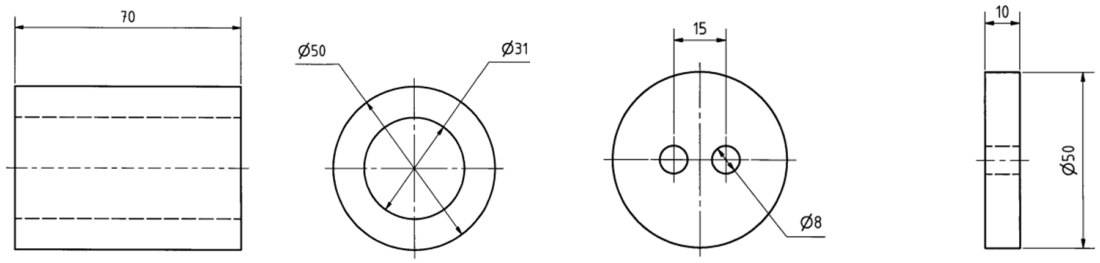

Figure 2-1 Teflon cylinder and specimen holder dimensions.

2.2.2 Rapid aging test

In addition to the immersion test outlined in the preceding section, the BigOxy test constitutes a sophisticated test method that has been developed to simulate the aging process of fuels and combustibles under accelerated conditions [5]. The process is founded on the principle of thermo-oxidative degradation, which involves the utilization of elevated temperatures and pressures to replicate the effects of long-term storage within a considerably shorter timeframe. The method is grounded in the principles of oxidation stability testing as outlined in ISO 16091 [6].

The available facility allows for the testing of larger fuel volumes, up to 2 liters, using 4 identical reactors, each with a capacity of 500 milliliters. During the testing process, samples are heated to 105°C and exposed to air at approximately 5 bar at start. The pressure and temperature levels are monitored to evaluate degradation behavior. The BigOxy system is capable of operation in two distinct modes. In the initial mode, the evaluation is concluded when a 10% pressure decline from maximum pressure is identified. This principle is analogous to the one employed in the RapidOxy method (ISO 16091). In the second mode, the test is executed for a predetermined duration, with the option to maintain a constant oxygen pressure by oxygen as needed.

In the context of this project, the latter mode was selected for the purpose of material compatibility testing, in conjunction with the long-duration test, as delineated in the preceding section. Due to the restricted availability of fuel, the decision was made to test several material specimens simultaneously in a single reactor. This approach was also conducted so as to maintain the ratio between the volume of test liquid and the surface area of the specimen (see previous section). For this purpose, selected glass containers were utilized and covered with a lid, allowing for pressure equalization (see Figure 2.2). Chapter Three details the particulars concerning the fuel and material samples that were subjected to testing in the four available reactors.

Following a four-week exposure period, a visual examination of the material specimens is conducted, and the alteration in weight is ascertained. The utilized blend is kept for the purpose of ICP-OES analysis, which is employed to quantify metal leaching (see section 2.2.4). Tensile testing was performed on the polymer specimens (see section 2.2.5).

Figure 2-2 Overview of BigOxi reactors and preparation of the different sample materials inside the reactors.

2.2.3 Hardware-in-the-loop

The hardware-in-the-loop (HiL) method is a flexible and cost-effective method for investigating the compatibility of fuel injection system components with a given fuel. In WP3, the compatibility of fuel components with MGO (Marine Gas Oil) and MGO-blends with different renewable HOEF fuel content was investigated. The investigation focused on a representative, modern common-rail diesel injection

system. The compatibility of the ether blends with the system's components is discussed in detail below, along with the resulting conclusions.

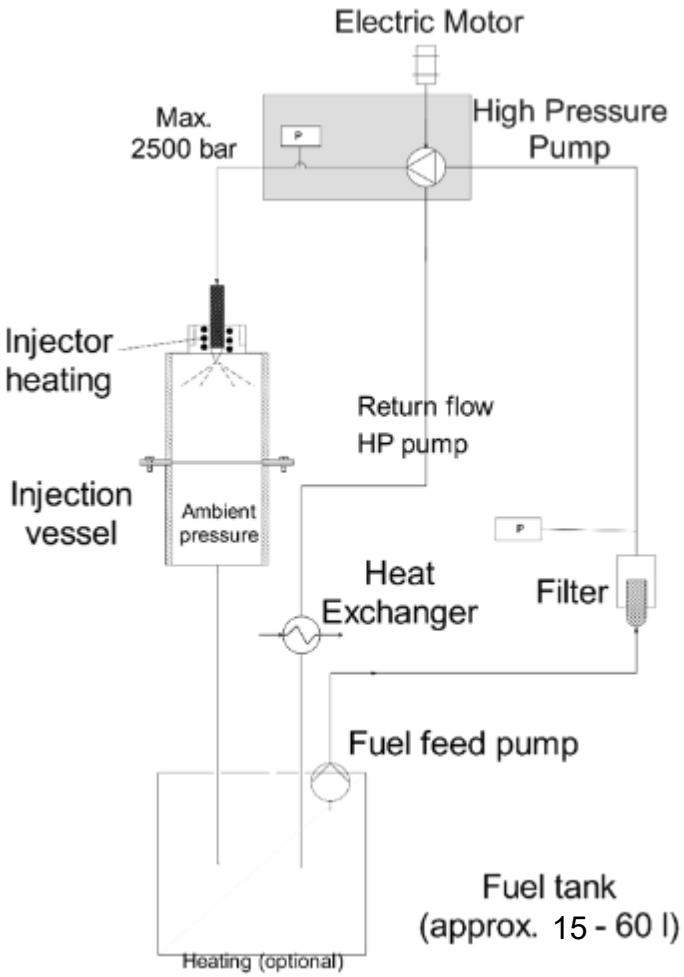

Figure 2-3 P&ID of the HIL test bench

The test principle of the hardware-in-the-loop method consists of connecting the components of the fuel injection system in a closed circuit that replicates the conventional application. Figure 2.3 shows the P&ID diagram of a HIL (Hardware-in-the-loop) setup. The fuel after injection is not ignited, but collected by condensing the fuel mist into the fuel tank. This allows 15 – 60 litres of fuel to be used and returned through the fuel-carrying components. The fuel, which is stressed by repeated flow through the components, accelerates the effects of material interactions. In this way, the compatibility of fuel and components can be determined in just 200 hours of cycle operation. In order to simulate the influence of combustion heat on the injection nozzle, the injection nozzle is additionally heated to the required temperatures determined from the application. The test cycles and test parameters are always selected in coordination with the parameters of the residual operation with only medium load range.

During the commissioning phase of the injection system, two batches of MGO were tested on the HIL test bench. These batches had a significant impact on the performance of the injection system. The

fuel batch, which will be referred to as 'poor quality fuel' for the remainder of this document, was provided by T4F for the commissioning phase and consisted of MGO blended with organic compounds to simulate marine oil containing additional bio-components. By contrast, the MGO fuel provided by Finco Energies, which will be referred as 'high-quality fuel' in the following and was also used for blending with the E-TANDEM surrogates, did not contain any additional components. The E-TANDEM blends used were kept for ICP-OES analysis to measure metal leaching (see the next section)

2.2.4 ICP-OES

As previously mentioned, during compatibility tests, materials are inspected for signs of corrosion, such as visible degradation, mass loss, or particle release into fuel. The application of Inductively Coupled Plasma Optical Emission Spectroscopy (ICP-OES) is a standard procedure for the detection of metal leaching [7].

ICP-OES is a highly sensitive and precise technique capable of detecting trace levels of metals released into the fuel during the test period. The use of ICP-OES allows for the measurement of elements such as iron (Fe), copper (Cu), zinc (Zn), aluminum (Al), nickel (Ni), and others. This analytical technique provides critical insight into the extent of corrosion and the stability of the material-fuel interface.

The technique relies on the generation of a high-energy plasma to excite atoms and ions in a sample. The plasma is produced by argon gas through a radiofrequency electromagnetic field, reaching temperatures between 5000 and 9000 Kelvin. At this temperature, the plasma possesses sufficient energy to atomize and excite the elements present in the sample.

The ICP-OES operates by subjecting a (digested) liquid sample to dilution, followed by atomization into a fine spray. This spray is then carried into the plasma using argon gas. Within the plasma, the substantial heat results in the excitation of the constituent atoms and ions of the sample. As these elements return to their ground state, they emit light at characteristic wavelengths, which are specific to each element. The emitted light is subsequently collected and separated by an optical system, such as a diffraction grating, and then measured by a sensitive detector. The intensity of the emitted light is directly proportional to the concentration of the corresponding element in the sample. By comparing these intensities with calibration standards, the concentrations of the elements can be precisely and accurately quantified.

Within this project the apparatus Agilent 5800 ICP-OES was employed. Regarding calibration standard the Conostan Multi-Element Standard S-21:100 pm was used, which contains following certified values: Ag, Al, B, Ba, Ca, Cd, Cr, Cu, Fe, Mg, Mn, Mo, Na, Ni, P, Pb, Si, Sn, Ti, V and Zn. Sample digestion was not part of the procedure, however some samples were measured externally, where digestion was included.

2.2.5 Tensile test

In order to test the impact of the fuels on the mechanical properties of the different fuel blends stretching tests according to DIN 53504 had been performed, see Figure 2.4. DIN 53504 is a German standard that outlines a procedure for testing the mechanical properties of rubber and elastomers, such as tear resistance, tensile strength, and elongation at break. The standard specifies the requirements for tensile testing, which involves stretching test specimens at a constant speed until they break, and then evaluating the recorded forces and strains. Based on ISO 37, the standard is used

throughout the rubber industry. The testing parameters met the requirements of DIN 53504, whereby the test specimens were clamped in place, preloaded at 50 mm/min to 0.1 MPa. Then they were stretched at 200 mm/min until they broke. The measurements were conducted using a Zwick Roell Z030 universal testing machine with a 1 kN force transducer. The length and force measurements are specified with Class 1 accuracy, corresponding to a measurement uncertainty of 1%.

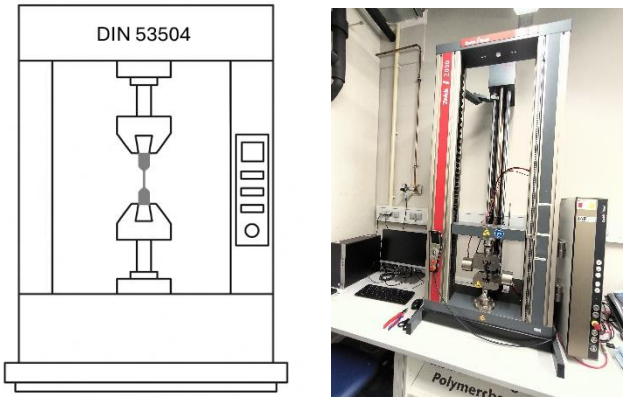

Figure 2-4 Test-Setup for DIN 54505 Testing of stretch testing of rubber and polymers (here Zwick Roell Z030)

2.3 Data Analysis

Most of the analyses performed yield direct numeric results, which are simply transferred into a consolidated overview. However, for certain instruments, the output requires additional explanation. Only the following case is of note:

Material Weight assessment: Material specimens were weighed several times as described in sections 2.2.1 and 2.2.2. A weighing was done threefold and an average determined. These average values were used to determine the weight change compared to the original weight before testing.

2.4 Overview on fuels and materials tested

An overview of the blends utilized for testing is provided in Table 2.1 below. It is noted that MGO-1[1] and MGO-2[1] refers different batches available. The MGO was in both cases used as provided, only stirred before usage.

Table 2.2 provides a comprehensive overview of the fuel quantities required for each type of analysis. Due to the limited availability of fuel, it was necessary to restrict most of the testing to the 10 and 20% ether blends. In the context of the adapted procedure pertaining to the rapid aging test (see section 2.2.2), it was found that a reduction in the requisite amount of fuel was possible. Consequently, the utilization of a 50% ether blend became a viable option.

[1] Kindly provided by FincoEnergies

Table 2.1 Overview of the blends availability for testing.

Fuel	Amount (Liter)	Remark
10% ether blend	30	Blend of 10% (v/v) ether HOEF surrogate-1 & 90% MGO-2
20% ether blend	30	Blend of 20% (v/v) ether HOEF surrogate-1 & 80% MGO-2
50% ether blend	0.7	Blend of 50% (v/v) ether HOEF surrogate-3 & 50% MGO-2

Table 2.2 Overview of the fuel volumes required per type of analysis test.

Analysis	Amount (ml)	Remark
Compatibility immersion test	6x500	6 refreshments included 4 metals, 2 polymers and blind sample
Big Oxy fast compatibility test	15-70	Depending on container size
HIL	15 000	Per fuel

The investigation involved the utilization of six distinct materials, including four metallic rods and two rubbers, which are often used in engines. Four primary metallic materials[2] are included:

- 42CrMo4: A chromium-molybdenum alloy steel known for its strength and moderate corrosion resistance,
- W-FA-55SiCr-QT-SP: A silicon-chromium alloy steel, usually used in spring applications,
- HS6-5-2: A high-speed tool steel with tungsten and vanadium, providing high hardness and wear resistance,
- 18CrNiMo7-6: A nickel-chromium-molybdenum alloyed case hardening steel, known for its toughness and fatigue strength.

The rods have a diameter of 8 mm, a length of about 10 cm and mass of about 80 grams, except for the W-FA-55SiCr-QT-SP which was available as a spring with an external diameter of 30 mm, wire thread thickness of 6.5 mm, total length of about 10 cm and weight of about 170 grams.

Additionally, two elastomers are included:

- FVMQ: Fluorosilicone Rubber is a silicone-based elastomer with added fluorine, offering superior resistance to fuel, oil and low temperatures.
- FKM: Fluoroelastomer is a high-performance synthetic rubber known for its excellent resistance to heat, chemicals and fuel, especially for automotive and aerospace environments.

Their geometry was available a flat dog bone with a thickness of 2 mm, total length of 7.5 cm and weight of about 5.5 (FVMQ) and 7.5 (FKM) grams.

[2] Kindly provided by WinGD Ltd.

As shown in Table 2.3, the materials under consideration contain specific elements that may leach into the liquid.

Table 2.3 Overview of the materials and their chemical composition for the corrosion test.

Material	C *	Si	Mn	P	S *	Cr	Mo	Ni	Cu	Al	V	W **	Fe
42CrMo4	X	X	X	X	X	X	X						X
W-FA-55SiCr-QT-SP	X	X	X	X	X	X			x				X
HS6-5-2	X	X	X	X	X	X	X				x	x	x
18CrNiMo7-6	x	X	X	x	x	x	x	x	x	x			x
FVMQ		X											
FKM													

* quantification in the liquid not possible with ICP-OES
**not in available Standard Calibration

3 Results & Discussion

This chapter presents and discusses the results of the fuel-component analyses performed according to the methodology provided in the previous chapter. First, the results of the compatibility immersion test are presented and discussed in section 3.1. Then the corresponding results for the rapid aging are covered in section 3.2. Finally, section 3.3 shows the results for the hardware-in-the-loop testing.

3.1 Compatibility immersion test

For the immersion test in total 14 containers were prepared, as shown in Table 3.1 and Figure 3.1. To ensure consistent orientation during evaluation, the upper part of each specimen rod was marked with a cross. In the figures below, the left side represents the bottom (fuel-immersed) section, while the right side represents the upper (vapor-exposed) section.

Table 3.1 Overview of the materials and their exposed fuel composition for the corrosion test.

	Material	Fuel	Remark
1	**42CrMo4**	10% ether surrogate	2 rods per container
2		20% ether surrogate	
3	**W-FA-55SiCr-QT-SP**	10% ether surrogate	1 spring per container, no Teflon parts
4		20% ether surrogate	
5	**HS6-5-2**	10% ether surrogate	2 rods per container
6		20% ether surrogate	
7	**18CrNiMo7-6**	10% ether surrogate	2 rods per container
8		20% ether surrogate	
9	**FVMQ**	10% ether surrogate	3 tensile samples per container
10		20% ether surrogate	
11	**FKM**	10% ether surrogate	3 tensile samples per container
12		20% ether surrogate	
13	**Teflon**	20% ether surrogate	Blind sample with Teflon
14	-	MGO-2	Blind sample with only fuel, added later

As described in the preceding chapter, weekly visual inspections were conducted. Throughout the duration of the testing period, no perceptible color change in the fuel was observed. However, black sediment was occasionally found at the bottom of the containers (see Figure 3.2, left and mid). The deposits in question are not believed to be related to corrosion; rather, they are likely contaminants originating from the MGO component.

This hypothesis is further substantiated by an additional observation: upon storing MGO in a 60°C oven for a period of one month (sample 14), the presence of dark sediments was noted within the fuel sample (Figure

3.2, right). The sediment observed in the compatibility test containers dispersed easily upon gentle agitation, further suggesting that it was non-metallic and not corrosion related.

Before delving into a more thorough exposition of the outcomes concerning the various materials of interest, it is imperative to acknowledge that sample 13, which contained the Teflon material, demonstrated no discernible alterations in its visual appearance or quantifiable mass over the course of the experimental period. This finding suggests that the material exhibited no significant corrosion or fuel absorption.

Figure 3-1 Overview of immersion test containers at start

Figure 3-2 Deposits on container bottom during monthly inspection, container 1, 6 and 14.

During the storage period, signs of corrosion were observed in metal 42CrMo4 as early as the first month under 60°C. A slight darkening of the sample was observed on both the fuel-immersed and vapor-exposed section of the rod, indicating that both the liquid and vapor phases of the fuel blend possess corrosive properties. By the 12-week mark, the darker discoloration had become clearly visible. Beyond this point, there were minimal further changes; however, both the upper and lower sections of the rod continued to show noticeable darkening (Figure 3.3). In the experiment involving an augmented ether surrogate concentration of 20%, 42CrMo4 exhibited a heightened propensity for corrosion. After the initial one-month period, a substantial black layer manifested on the lower, fuel-immersed segment of the rod, thereby signifying substantial material degradation. The area that had been exposed to vapor exhibited indications of corrosion, albeit to a lesser extent. The discoloration is likely attributable to surface oxidation or mild interaction with ether components in the fuel. These effects appear to be confined to the surface and are not indicative of significant damage to the material. Mass measurements were conducted at the beginning of the study and at regular monthly

intervals. These measurements revealed no statistically significant variations within the range of measurement uncertainty, which was set at 0.1%.
After the mass change evaluation, an ICP-OES analysis was conducted to detect any metal ions released into the fuel during the immersion process. The objective of this study was to assess the occurrence of corrosion or leaching of metallic elements. The results demonstrated that the presence of typical metallic elements, such as iron (Fe) and chromium (Cr), was not detected in the fuel post-testing. This observation is consistent with the mass measurements and visual inspections, which confirm that the metallic rods remained chemically stable in the 10% and 20% ether surrogate and did not undergo measurable corrosion or degradation during the exposure period.
The overall assessment remains satisfactory, with the observed corrosion levels deemed acceptable.

The spring steel (W-FA-55SiCr-QT-SP) exhibited remarkable corrosion resistance under the conditions of the test. Despite a six-month exposure period, no observable changes were detected on the metal surface. The material demonstrated stability and resistance to degradation in both fuel environments, indicating a high level of chemical stability and durability (Figure 3.4). No substantial alterations were observed. In addition, the ICP-OES (Inductively Coupled Plasma-Optical Emission Spectrometry) analysis revealed no evidence of metal leaching into the fuel.

Figure 3-3 42CrMo4 with increasing immersion time in 10% (left) and 20% (right) ether surrogate (left fuel-immersed, right vapor-exposed section).

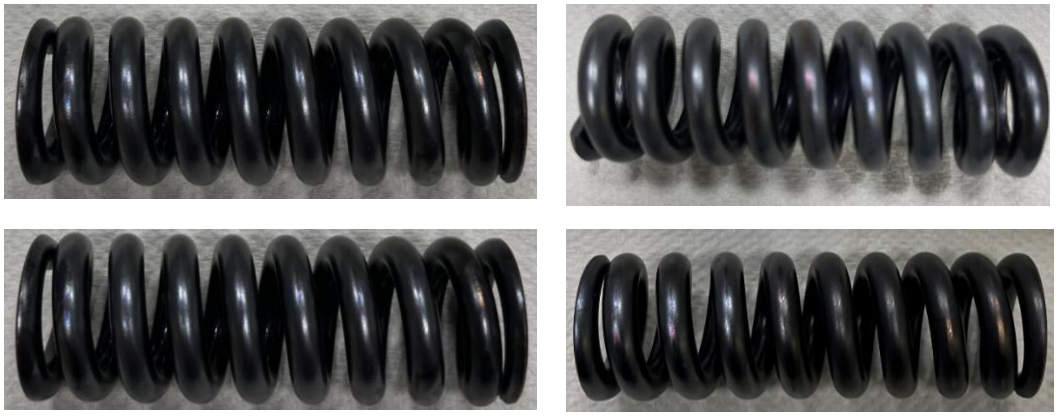

Figure 3-4 W-FA-55SiCr-QT-SP with increasing immersion time in 10% (left) and 20% (right) ether surrogate (left fuel-immersed, right vapor-exposed section).

HS6-5-2 high-speed steel demonstrated analogous corrosion resistance behavior to that of the spring steel in the 10% ether surrogate blend. Following a six-month exposure period, no observable surface degradation or discoloration was detected (see Figure 3.5). HS6-5-2 steel demonstrated negligible surface darkening following one month of exposure to the 20% ether surrogate blend. The corrosion exhibited a moderate progression over the course of the six-month period. However, the discoloration remained relatively confined and did not progress to severe blackening. It is noteworthy that signs of corrosion were also observed on the vapor-exposed portion of the sample. This finding indicates that the ether-containing fuel blend exhibits a slight corrosive effect, both in the liquid phase and in the vapor phase. No substantial alterations were detected in this instance. Moreover, the ICP-OES (Inductively Coupled Plasma-Optical Emission Spectrometry) analysis revealed no evidence of metal leaching into the fuel. The overall impression remains satisfactory, and the observed corrosion is deemed acceptable.

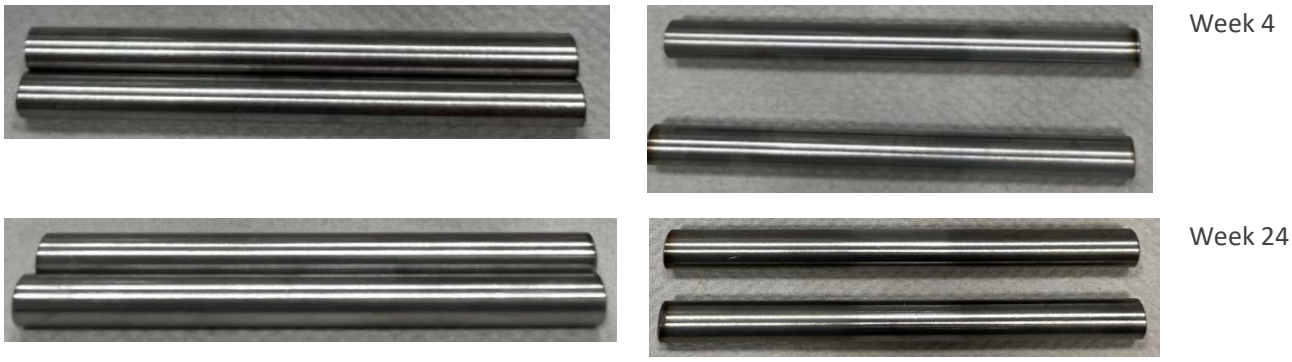

Figure 3-5 HS6-5-2 with increasing immersion time in 10% (left) and 20% (right) ether surrogate (left fuel-immersed, right vapor-exposed section).

Figure 3-6 18CrNiMo7-6 with increasing immersion time in 10% (left) and 20% (right) ether surrogate (left fuel-immersed, right vapor-exposed section).

The steel grade 18CrNiMo7-6 demonstrated slight surface darkening following a six-month exposure period, suggesting the initiation of mild corrosion (see Figure 3.6). In the 20% ether surrogate, 18CrNiMo7-6 exhibited accelerated and more substantial corrosion. By the conclusion of the initial month, the fuel-immersed segment of the specimen had already undergone a discernible darkening. By the sixth month, the corrosion had intensified significantly, with a dark layer covering the lower part of the rod. The findings indicate that 18CrNiMo7-6 is more prone to corrosion in ether-containing fuel blends, particularly in the liquid phase. However, the overall impression remains satisfactory, and the observed corrosion is deemed acceptable. No substantial alterations were detected, and the ICP-OES examination revealed no indications of metal contamination in the fuel.

With regard to the elastomeric materials (FVMQ and FKM) over the course of the exposure period, no observable cracking or severe surface degradation was observed on either material, irrespective of the ether concentration. FKM exhibited no discernible change in appearance, while FVMQ demonstrated a marked darkening of its coloration, ultimately acquiring a brown hue by the conclusion of the six-month period (Figure 3.7). This discoloration suggests the presence of chemical interactions with the fuel blend.

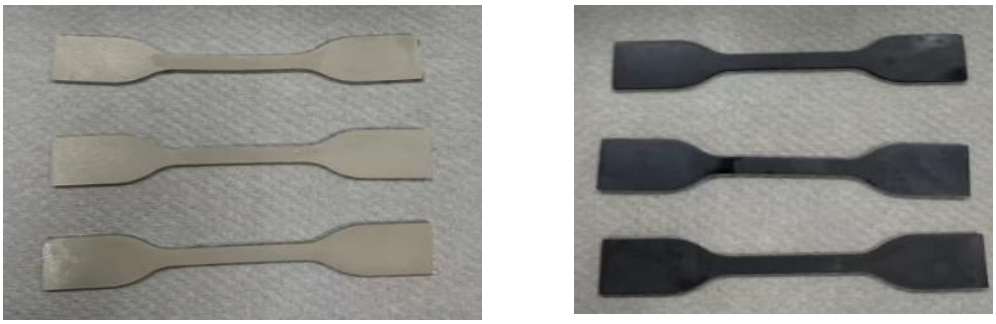

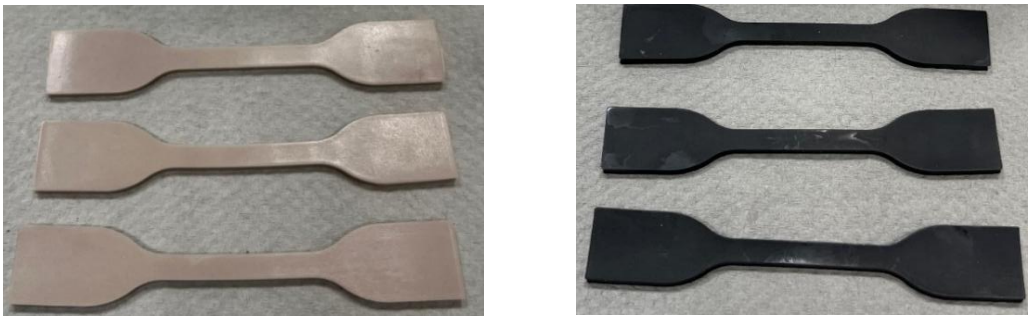

Figure 3-7 FVMQ (left) and FKM (right) with increasing immersion time in 20% ether surrogate (left fuel-immersed, right vapor-exposed section).

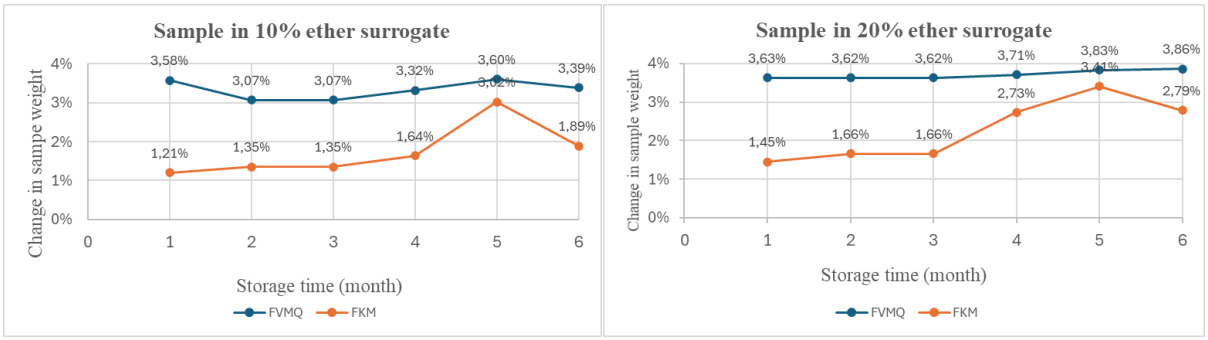

Figure 3-8 FVMQ and FKM relative weight change with increasing immersion time in 10% (left) and 20% (right) ether surrogate.

In contrast to the metals, the two elastomeric materials, FKM and FVMQ, exhibited evident alterations in mass over time. The monthly mass measurements were expressed as a percentage relative to each sample's original weight, revealing a significant increase in weight. As demonstrated in Figure 3.8, FVMQ experienced a substantial increase in weight during the initial one-month period in the 10% ether surrogate blend, exhibiting a mass change of 3.58%. In the subsequent weeks, the mass exhibited a slight decrease, yet it remained higher than the initial level, concluding at 3.39% after a six-month period. This observation suggests that the rubber absorbed fuel at an accelerated rate during the initial phase. Subsequent minor alterations indicate that the material attained a state of equilibrium, with minimal further absorption or release of fuel. The 20% ether surrogate blend exhibited a similar trend, with FVMQ absorbing fuel at a rapid rate, beginning at 3.63% in the first month and reaching 3.86% by the sixth month.

In the 10% ether surrogate blend, FKM demonstrated an increase in weight, although it was less than that observed for FVMQ. The data demonstrated an initial percentage of 1.21% in the first month, which gradually increased to 3.02% by the fifth month. Subsequently, there was a decline to 1.89% by the sixth month. In contrast to the rapid response exhibited by FVMQ, FKM demonstrated a more gradual and consistent uptake. This slow mass gain also points to swelling, but at a lower and more gradual rate. The behaviour of FKM in the 20% ether blend does not deviate much from the 10% ether blend. The mass increased from 1.45% in week one to 2.79% by month six. This behavior indicates slower fuel absorption compared to FVMQ, as was also observed in the 10% ether test.

As indicated by the data, a slight decrease in mass was observed in both elastomer samples at the fourth month in comparison to the third month. This decline may be attributed to either partial fuel desorption or surface evaporation. Another potential explanation pertains to the fuel change, which

has the potential to temporarily disrupt the equilibrium between the rubber and the fuel. After this, both materials exhibited an increase in weight during week five, indicating a re-establishment of fuel absorption or a period of stability in the new fuel.

After the mass change evaluation, an ICP-OES analysis was conducted to detect any metal ions released into the fuel during the immersion process. In the case of the polymers, silicon was found to be leached. Fuel samples obtained from rubber immersion tests demonstrate that FVMQ releases a significantly higher quantity of silicon into the fuel compared to FKM. As illustrated in Figure 3.9, the concentration of silicon (in ppm) detected in the fuel after each month was examined for both FVMQ and FKM in 10% and 20% ether surrogate blends. As indicated by the findings of the study, the value for FVMQ obtained a peak of approximately 31 and 44 ppm after the first month for the 10 and 20% blend, respectively. The amount of Si leached into the fuel underwent a gradual decrease over exposure time.
In comparison, FKM demonstrated minimal silicon release across all conditions. The Si concentration demonstrated negligible variability, maintaining its range from 1 to 2 ppm, irrespective of the fuel blend ratio or the duration of storage (Figure 3.9).

These findings indicate that FVMQ is more prone to leaching silicon into the fuel, particularly during the early stages of exposure. This behavior is attributed to its silicone-based composition, which contains a high proportion of silicon within its polymer structure. Conversely, FKM is predominantly carbon-based and contains a negligible amount of silicon, leading to a substantial reduction in leaching. It is noted that carbon cannot be measured with the ICP-OES method.
FVMQ turns up in diesel systems where parts must stay supple in deep-cold but still tolerate fuel splash, vapor, or occasional wetting. It can be found on cold-climate vehicles and gensets in places like tank-vent and rollover valves, breather/check valves, filler-cap seals, quick-connector O-rings, and delicate diaphragms in pressure or purge/vent valves, i.e. spots that see diesel mist or intermittent contact rather than continuous soak. In forecourt equipment the same logic applies: dispenser nozzles, swivels, and meter heads in Nordic-style winters often use FVMQ seals so they don’t harden and leak when temperatures plunge. The release of silicon from FVMQ may have implications for long-term material stability and could potentially affect fuel purity over time, advising for the use of alternative elastomers for parts with prolonged soak times with ether HOEF-containing fuel blends

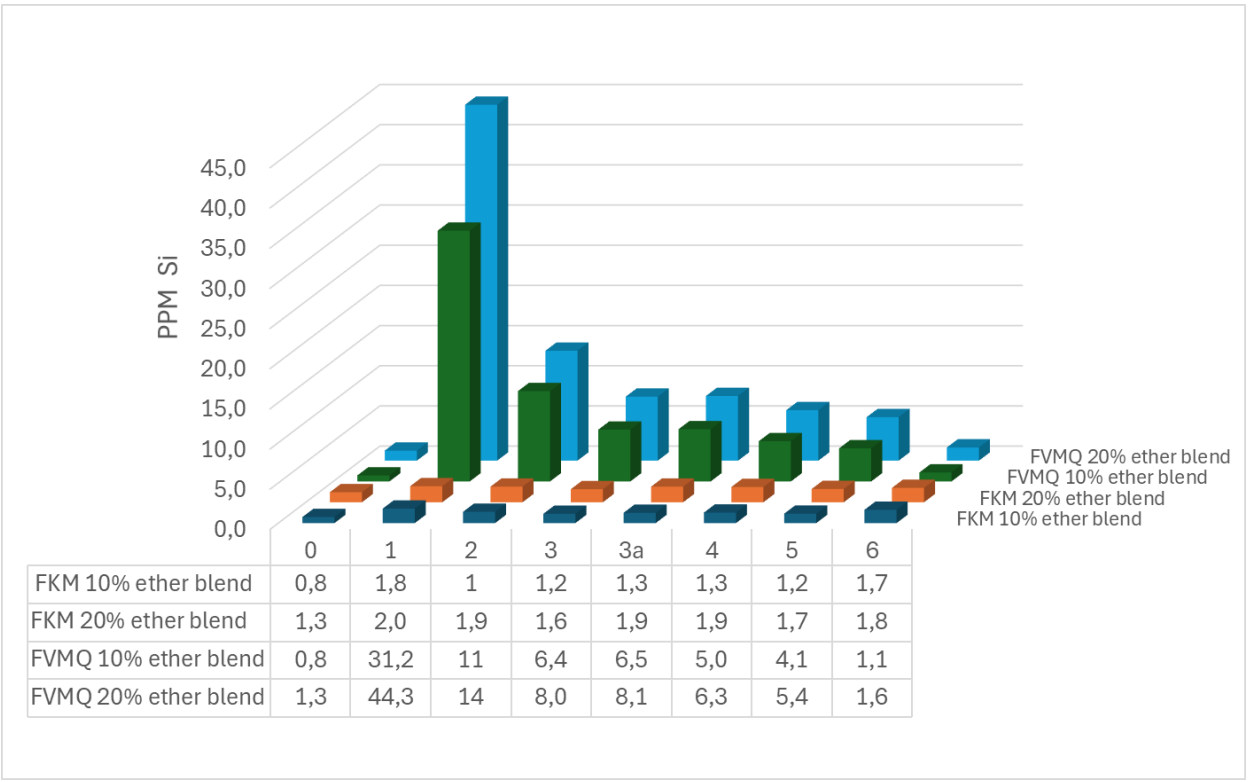

	0	1	2	3	3a	4	5	6
FKM 10% ether blend	0,8	1,8	1	1,2	1,3	1,3	1,2	1,7
FKM 20% ether blend	1,3	2,0	1,9	1,6	1,9	1,9	1,7	1,8
FVMQ 10% ether blend	0,8	31,2	11	6,4	6,5	5,0	4,1	1,1
FVMQ 20% ether blend	1,3	44,3	14	8,0	8,1	6,3	5,4	1,6

Figure 3-9 FVMQ and FKM silicon release into the fuel over the test period of 6 months.

Furthermore, tensile stress tests were conducted to measure the impact of the fuel blends after six months of aging. The samples were tested according to DIN 53504, as described in Chapter two. In Figure 3-10, the test results for FKM and FMVQ samples with different blend compositions. For the 10% and 20% blends, the FMVQ material shows a slightly reduced the stiffness. However, tensile strength at break is significantly reduced. For FKM, stiffness remains almost unchanged; however, the nonlinear elastic region at the beginning of the test is more affected, leading to lower stress for the same strain up to 22%. The tensile strength is slightly higher than that of the baseline material.

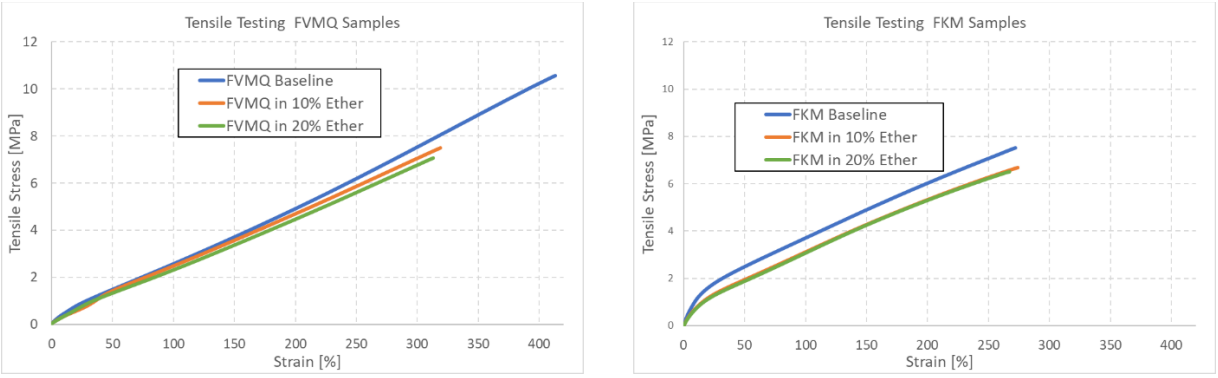

Figure 3-10 Results of the Tensile Streng Tests for FVMQ and FKM after 6 months aging

3.2 Rapid aging test

In light of the findings from the extensive testing process outlined in the preceding section, it was determined that a more rigorous evaluation was necessary to ascertain the material's endurance

capacity when subjected to the e-fuel. The elevated temperature of 100°C was employed in the simulation, which translates to a lifetime equivalent to approximately 16 times that of the 6-month compatibility test described in the previous section. This increase is consistent with the established guideline that a 10°C increase in temperature results in a doubling of the reaction speed and thus the simulated lifetime (Van 't Hoff Equation [8]). An increase in temperature also results in oxidation, which in turn exacerbates the severity of the test.

An overview of the selected materials is provided in Table 3.2. Due to the limited availability of reactors at the BigOxy test rig, the 10% ether surrogate was not investigated. One reactor was utilized for the 50% ether surrogate-3 blend, the others with the 20% ether blend. The present study was only able to test the four materials that were selected based on the results of the 6-month compatibility test.

Table 3.2 Overview of the materials and their exposed fuel composition for the rapid aging test.

	Material	Fuel	Remark
1	**W-FA-55SiCr-QT-SP**	20% ether surrogate	Reactor 1 (spring material in 70ml fuel)
2	**42CrMo4**	20% ether surrogate	Reactor 2 (Rod 1 in 15 ml fuel)
3	**18CrNiMo7-6**	20% ether surrogate	Reactor 2 (Rod 2 in 15 ml fuel)
4	**HS6-5-2**	20% ether surrogate	Reactor 2 (Rod 3 in 15 ml fuel)
5	**FKM**	20% ether surrogate	Reactor 3 (in 15 ml fuel)
6	**FKM**	20% ether surrogate	Reactor 3 (in 15 ml fuel)
7	**FVMQ**	20% ether surrogate	Reactor 3 (in 15 ml fuel)
8	**FVMQ**	20% ether surrogate	Reactor 3 (in 15 ml fuel)
9	**42CrMo4**	50% ether surrogate	Reactor 4 (Rod 4 in 15 ml fuel)
10	**18CrNiMo7-6**	50% ether surrogate	Reactor 4 (Rod 5 in 15 ml fuel)
11	**FKM**	50% ether surrogate	Reactor 4 (in 15 ml fuel)
12	**FVMQ**	50% ether surrogate	Reactor 4 (in 15 ml fuel)

Figure 3-11 W-FA-55SiCr-QT-SP before (left) and after (right) BigOxi testing in 20% ether surrogate (left fuel-immersed, right vapor-exposed section).

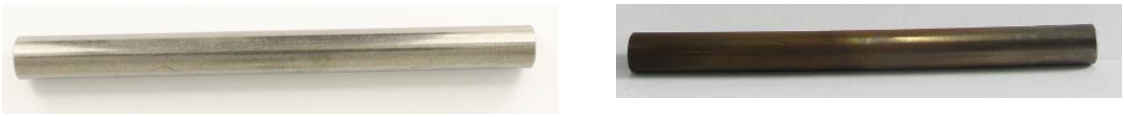

Figure 3-12 42CrMo4 before (left) and after (right) BigOxi testing in 20% ether surrogate (left fuel-immersed, right vapor-exposed section).

Figure 3-13 18CrNiMo7-6 before (left) and after (right) BigOxi testing in 20% ether surrogate(left fuel-immersed, right vapor-exposed section).

Figure 3-14 HS6-5-2 before (left) and after (right) BigOxi testing in 20% ether surrogate (left fuel-immersed, right vapor-exposed section).

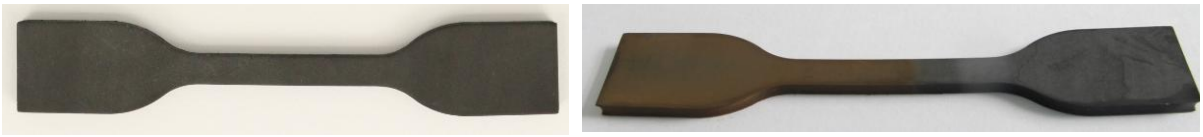

Figure 3-15 FKM before (left) and after (right) BigOxi testing in 20% ether surrogate (left fuel-immersed, right vapor-exposed section).

Figure 3-16 FVMQ before (left) and after (right) BigOxi testing in 20% ether surrogate (left fuel-immersed, right vapor-exposed section).

Figure 3-17 42CrMo4 before (left) and after (right) BigOxi testing in 50% ether surrogate (left fuel-immersed, right vapor-exposed section).

Figure 3-18 18CrNiMo7-6 before (left) and after (right) BigOxi testing in 50% ether surrogate (left fuel-immersed, right vapor-exposed section).

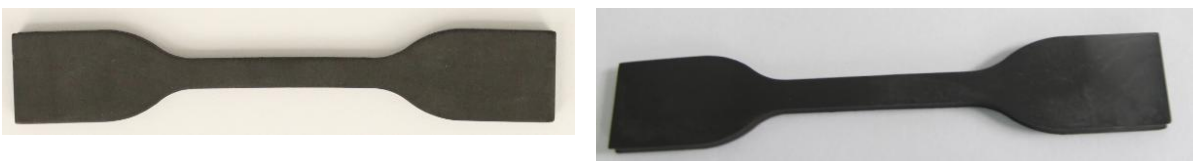

Figure 3-19 FKM before (left) and after (right) BigOxi testing in 50% ether surrogate (left fuel-immersed, right vapor-exposed section).

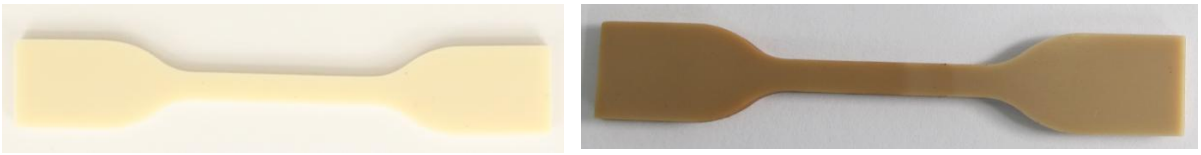

Figure 3-20 FVMQ before (left) and after (right) BigOxi testing in 50% ether surrogate (left fuel-immersed, right vapor-exposed section).

As demonstrated in Figure 3.11-20, a visual impact is observed for all materials. The degree of impact for the metals is elevated in comparison with the 6-month compatibility test; nevertheless, for the 20% ether blend, it remains within acceptable limits, since as addressed below, no leaching and mass change occurred. The most significant impact was observed on the metal rod 18CrNiMo7-6 in the 50% ether blend, as evidenced by the presence of small corrosion pits. An examination of the metal samples revealed no discernible alteration in their weight.

The visual alterations on the polymers are now also distinctly discernible on the FKM, particularly for the 20% ether blend. As was the case in the 6-month duration test (see previous section), the weights have undergone changes, as illustrated in Figure 3.21. A similar set of alterations was identified in the FVMQ and the 20% ether blend. Nonetheless, the exposure to the 50% blend demonstrated a value that exceeded 7%. A more noteworthy observation is the weight increase of up to 11% observed in the FKM material. It has been posited that the alterations observed in this rapid aging test exerts a greater effect on the FKM than on the FVMQ. A conspicuous increase in values is evident when compared to the 6-month comparability test for the FKM elastomer. However, it is imperative to acknowledge that the number of specimens examined is limited, given the substantial variation observed between the two specimens in the 20% blend.

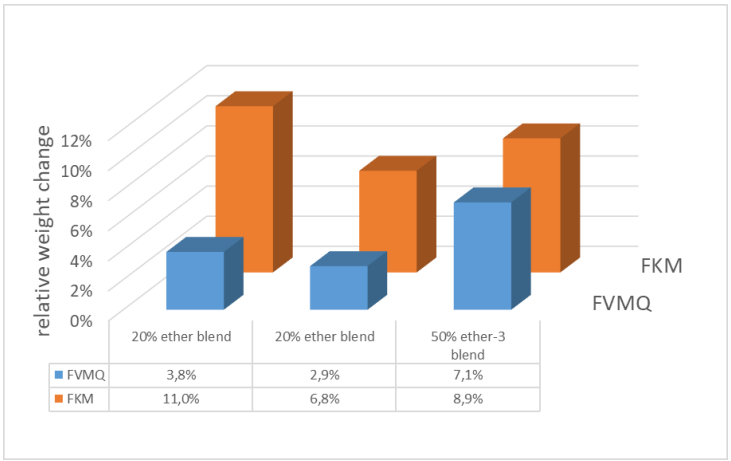

Figure 3-21 FVMQ and FKM relative weight change.

ICP-OES was performed on the HOEF to verify the leaching process once more. As was the case previously, no metals were found to have any significant concentrations. The silicon concentrations of the fuel from the polymer tests are displayed in Table 3.3. The findings indicate that the Si-content of the FVMQ material exceeds that of the FKM material. The values are elevated in comparison to the 6-month comparability test, not solely for the monthly values (subsequent to which the fuel was invariably replenished) but also for the aggregate of the entire 6-month period. This outcome serves

to underscore the severity of the rapid aging test. However, there is some suspicion that Si leached from the glass container used in this testing. Therefore, it is hypothesized that a dummy container with only fuel should have been enclosed in the test. It is evident that an increase in the ether content results in an enhancement of the value of FKM. However, the impact on the FVMQ material is not immediately apparent. This could be indicative of a complete leaching of free silicon.

Table 3.3 Overview of the Si leaching for the polymer materials after the rapid aging test.

	Material	Fuel	Silicon (mg/kg)
5	**FKM**	20% ether surrogate	54
6	**FKM**	20% ether surrogate	84
7	**FVMQ**	20% ether surrogate	140
8	**FVMQ**	20% ether surrogate	240
11	**FKM**	50% ether surrogate	140
12	**FVMQ**	50% ether surrogate	200

Also, tensile strength tests have been conducted on the samples with rapid aging under the same boundary conditions previously discussed for the long-duration tests. Figure 3-22 shows the test results for FKM and FMVQ samples with different blend compositions. In addition to two tensile stress measurements of the 20% blend after rapid aging, the tensile stress for the 20% blend after long-duration aging has been included. Note that the material properties are significantly affected by the aging method. For rapid aging, the non-linear elasticity region exhibits lower stresses for the same strain. The stiffness of both materials is also lower. Interestingly, the tensile strength is higher for the rapid-aged 20% ether blend than for the samples aged over a long duration. For FKM, the tensile strain is higher than that of the baseline material. In the rapid aging investigations, a 50% blend was also examined. For FVMQ, the stiffness and tensile strength are significantly reduced. For FKM, the stiffness and tensile strength are the same as the 20% blend.

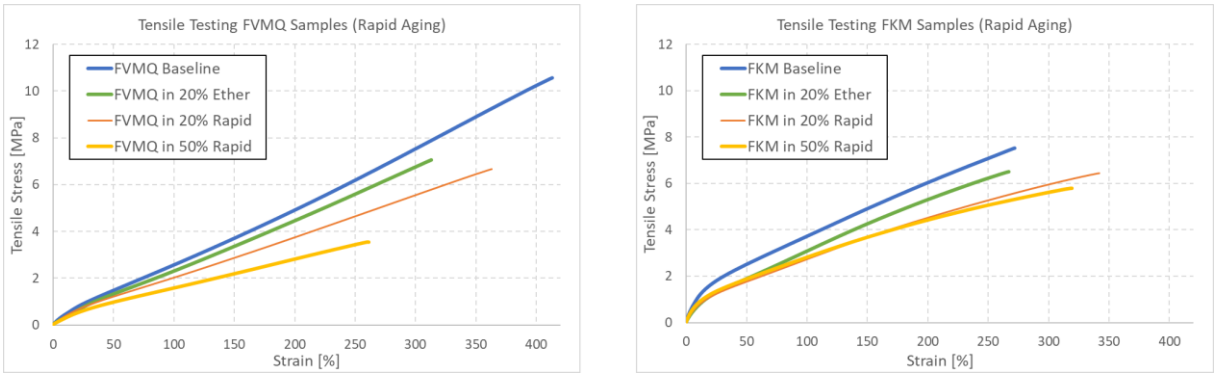

Figure 3-22 Results of the Tensile Streng Tests for FVMQ and FKM after rapid aging.

3.3 Hardware-in-the-loop test

To evaluate the fuel injection compatibility of MGO–Ether blends, Hardware-in-the-Loop (HiL) measurements were performed on Tec4Fuel's test bench, (Figure 3-23). A conventional solenoid-type common-rail fuel injection system was employed to carry out 200-hour durability tests under medium-load conditions.

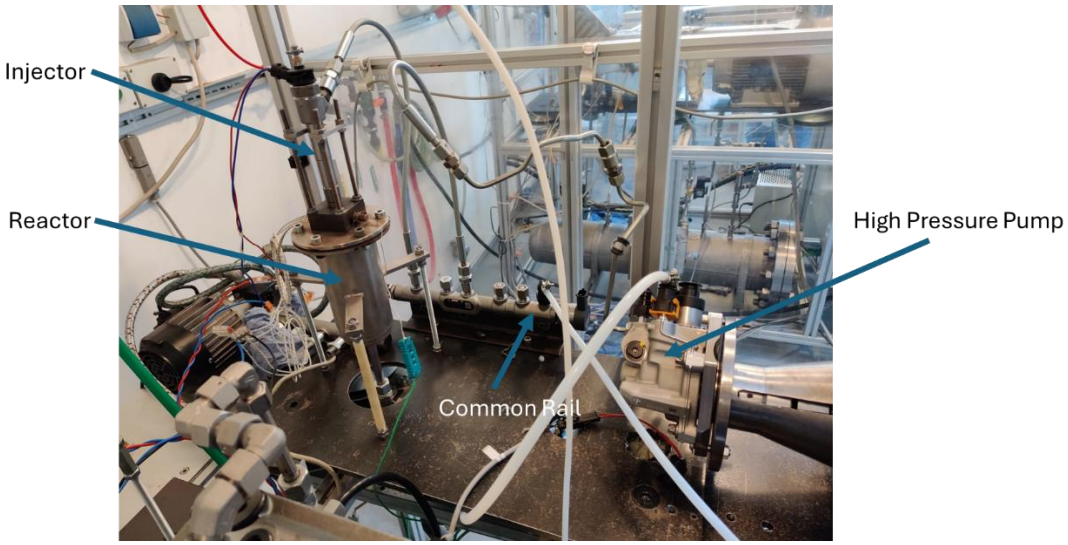

Figure 3-23 Hardware in the Loop-Testbench used for the injection system evaluation for the different blends.

During the commissioning phase with injector 1, low-quality marine gas oil (MGO) was used. This resulted in significant injector coking after only 50 hours of operation. For subsequent investigations, a new injector (Injector 2) was installed, and three fuels were tested: high-quality MGO, a 20% MGO–ether blend, and a 10% MGO–ether blend. A modern common-rail injection system, which is typically used in light commercial vehicles and small marine engines, was used for the investigation. The smaller nozzle holes of these injectors capture and amplify the effects of coking (deposits on the injector tip and nozzle holes) resulting from poor fuel quality and composition. Figure 3-24 shows a picture of the injector and the nozzle tip, revealing the small nozzle holes through which the fuel is injected into the chamber.

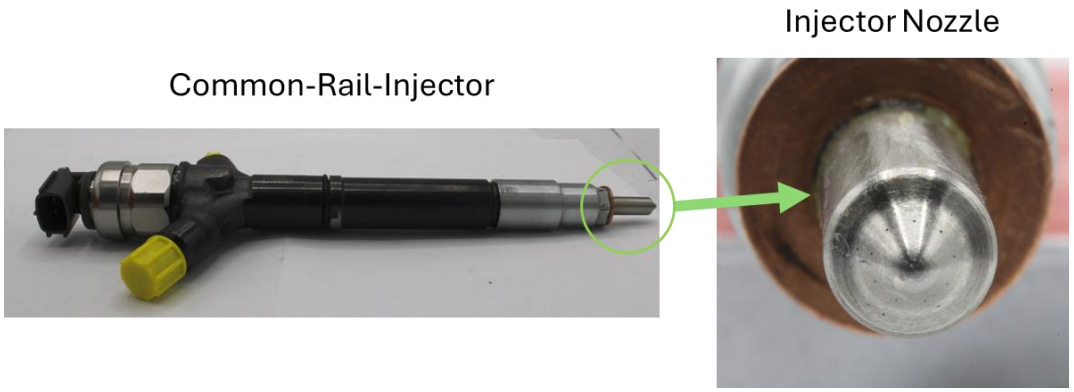

Figure 3-24 Common-rail injector and injector nozzle used for the HiL-tests.

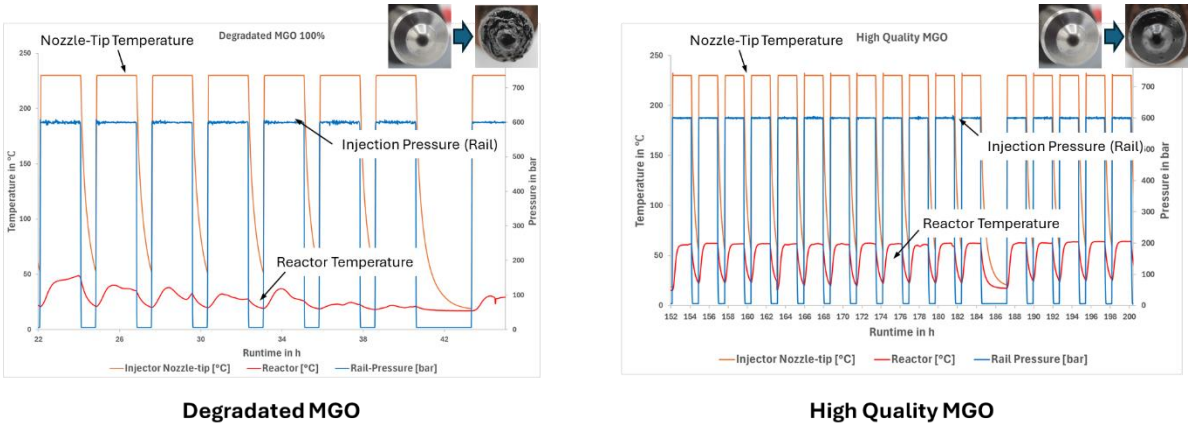

Degradated MGO **High Quality MGO**

Figure 3-25 Comparison of HiL performance for degradated MGO and high quality MGO.

The injection system has been tested for over 200 hours with different fuels. To simulate combustion conditions at the nozzle tip, the nozzle is heated electrically to 230°C. During the test, the rail pressure, nozzle tip temperature, and reactor temperature are monitored. A reduction in reactor temperature indicates deterioration of the nozzle, as less fuel is getting through the nozzle holes.

Figure 3-25 shows a comparison of poor-quality and high-quality MGO. The lower diagram on the left shows the temperature loss over time. A picture of the nozzle also shows the large amount of deposits on its top. On the right, a high-quality MGO fuel test is shown. In this case, the temperature in the reactor shows no deterioration because few deposits are generated at the nozzle.

Subsequently, the base fuel (MGO) and the two MGO-ether blends were tested with the same injector to minimize the effects of hardware dispersion. The fuel injection lines were cleaned after each test. All three fuels showed no significant degradation in injector flow performance, as there was no degradation in the reactor temperature. However, an interesting cleaning effect of the nozzle was observed with the 20% Ether-blend after the MGO baseline, as deposits from the previous fuel tests had detached (small black flakes), **Fout! Verwijzingsbron niet gevonden.**. Therefore, the ether blend has fuel-cleaning capabilities that are beneficial for injection system durability. The flakes were removed before testing the 10% ether blend. The flow performance of the 10% blend did not deteriorate. Deposits on the nozzle tip were observed, though slightly less than with 100% MGO.

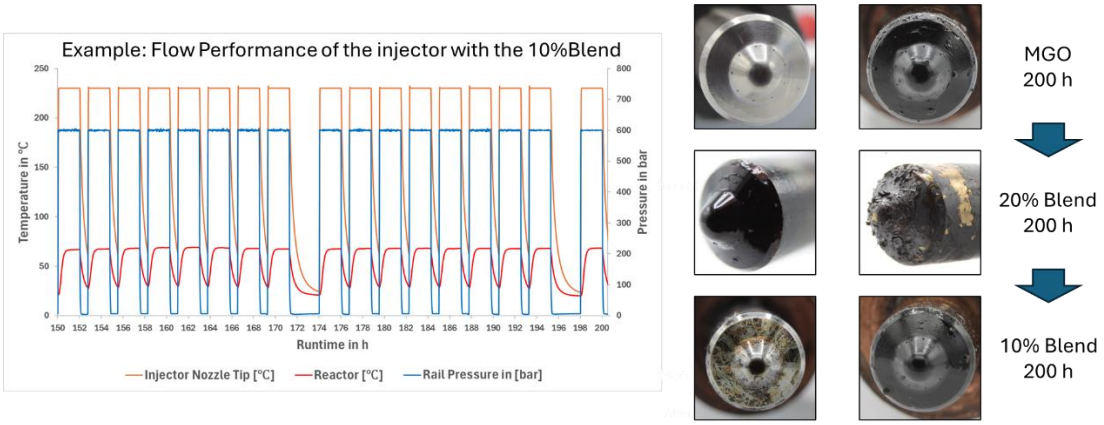

Figure 3-26 Impact of fuel composition and nozzle coking.

3.4 Contribution to project (linked) Objectives

The results included in this report contribute to the achievement of the following project objectives:

Objective 4. To characterize the newly proposed higher oxygenate e-fuel (HOEF) in its two realizations i.e. a mixture of either higher aliphatic alcohols or higher aliphatic ethers, and assess its drop-in characteristics for current-fleet marine and heavy-duty road internal combustion engines. This comprises:

Subobjective (4a) to design blending strategies with baseline fuels, and additivation to attain drop-in and backwards compatibility with reference to ISO8217 and EN590 current regulations for marine and road heavy-duty diesel fuels.

Subobjective (4b) to assess the compatibility of selected formulae of the higher oxygenate e-fuel with the existing fuel supply systems and current fleet internal combustion (IC) diesel engine though fit-for-purpose corrosion, oxidation, hygroscopicity, and hardware-in-the-loop material-fuel compatibility test using limited amounts of fuel (<25 dm^3).

Given the focus of the project on e-fuel applications in waterborne transport, Marine Gasoil (MGO) has been selected as a relevant baseline fuel.

3.5 Contribution to major project exploitable result

The results included in this report identify the best state of the art purification method. As such these results contribute to attaining the following Key Exploitable Result:

KER	Fuel characterization
Owner	OWI, T4F
Alternative solution/Market Competition	Other research institutes in this area
Use model to go to the market	Provision of a service
Potential End user/market	Shipping industry, transport industry, e-fuel end users in general
Target market/companies	Fuel development, fuel production and fuel trade companies
Unique selling point	Knowledge on similar fuels, special self-developed methods and equipment
Time to go market	Immediately
Steps to facilitate exploitation	Publications
Risk evaluation	Political change on climate policy: P: 30%, I: 50%, R=15%

4 Conclusion and Recommendation

The present study evaluated the compatibility of various metallic and elastomeric materials with fuel blends containing 10%, 20% and 50% (w/w) ether surrogate. Among the metals, 42CrMo4 and 18CrNiMo7-6 exhibited some acceptable corrosion, particularly in the higher concentration, while other metals demonstrated negligible or no corrosion over the 6-month test period. In the more severe rapid aging test, corrosion was observed in all materials. However, the results were still deemed acceptable for the 20% ether blend test, since no weight change and leaching was found. A study was conducted to determine the corrosion resistance of 18CrNiMo7-6 in the presence of 50% ether blend. The results indicated the presence of pitting corrosion in the 18CrNiMo7-6 sample.

The elastomer FVMQ exhibited significant darkening over time in both tests conducted. A visual change in the elastomer FKM was only observed after the rapid testing. Both elastomers demonstrated a propensity to absorb fuel and undergo an increase in mass. In the 6-month soaking test under ambient conditions, FVMQ exhibited a faster and more pronounced mass uptake, while FKM exhibited a substantial mass increase only in the rapid aging test.

ICP-OES analysis showed that FVMQ released silicon into the fuel, suggesting chemical interaction and potential impact on long-term material and fuel stability.

Hardware-in-the-Loop (HiL) tests were conducted using a test bench to assess the compatibility of marine gas oil (MGO)–ether blends with a common-rail fuel injection system. Initial tests with low-quality MGO caused severe injector coking after 50 hours, prompting further evaluation with high-quality MGO and MGO–ether blends (10% and 20%). Over 200-hour durability tests under medium-load conditions, injector performance was monitored by measuring rail pressure, nozzle temperature, and reactor temperature. High-quality MGO showed stable performance with minimal deposits, while low-quality MGO caused significant coking and temperature drop. The ether blends demonstrated good injector compatibility with no degradation in flow performance, and the 20% ether blend even exhibited a cleaning effect, removing previous deposits—indicating its potential benefits for injection system durability.

Based on the results of the investigations reported here, it is concluded that the goal of rapid market introduction of e-fuels with higher oxygen content (HOEF) is achievable, especially when ether-based HOEFs are blended with conventional fuels such as MGO.

5 Risks and interconnections

5.1 Risks/problems encountered

Risk No.	What is the risk	Probability of risk occurrence[1]	Effect of risk[1]	Solutions to overcome the risk
WP 3.1	Low flash point	1	2	Improve within the production process, otherwise blend with suitable fuel
WP 3.2	High water content for the HOEF and its blends	1	3	For waterborne transport, check for each fuel charge, so that ship's captain can decide whether water content and energy density is acceptable for the intended voyage.
WP 3.3	FVMQ seal failure	2	1	Avoidance of FVMQ or regular seal replacement

[1)] Probability risk will occur: 1 = high. 2 = medium. 3 = Low

5.2 Interconnections with other deliverables

Report	Interconnection
D2.1 and D2.4	Describe the production of the HOEF ether surrogate analysed and tested in D3.1. D3.2 and D3.3
D3.1	Whereas the present D3.3 summarizes all fuel-system compatibility trials and hardware-in-the-loop aging tests results, earlier D3.1 reported on the fuel physicochemical properties.
D3.2	Whereas the present D3.3 summarizes all fuel-system compatibility trials and hardware-in-the-loop aging test results, D3.2 complements D3.1, reporting results from investigations on the fuel ignition and soot formation profile.

6 Deviations from Annex 1

There are no deviations from the description of this deliverable as given in Annex I of the Grant Agreement.

7 References

1. Beständigkeit gegen Korrosion metallischer Werkstoffe durch Kraftstoffe, VDA-230-207, https://www.ima-dresden.de/norm/vda-230-207/, Januar 2008
2. Hoffmann, H., Lucka, K. (2019). Hardware-in-the-loop testing: Complete Common Rail System (CoCoS) and component testing as rapid and cost-efficient tool in the introduction of alternative fuels in the automotive sector. In: Tschöke, H., Marohn, R. (eds) 11. Tagung Einspritzung und Kraftstoffe 2018. Proceedings. Springer Vieweg, Wiesbaden. https://doi.org/10.1007/978-3-658-23181-1_18
3. Mineralölerzeugnisse - Korrosionswirkung auf Kupfer – Kupferstreifenprüfung, DIN EN ISO 2160:1999-04, https://dx.doi.org/10.31030/8069636, April 1999
4. Standard Test Method for Rust-Preventing Characteristics of Inhibited Mineral Oil in the Presence of Water, ASTM D665-06 135/93
5. S. Sriram: Standardization of Bigoxy method for e-fuel like methanol, gasoline, and their blends. Instituto Superior Tecnico, Universidade de Lisaboa, Portugal, October *2022*
6. Flüssige Mineralölerzeugnisse - Mitteldestillat- und Fettsäure-Methylester (FAME)-Kraftstoffe und -Mischungen - Bestimmung der Oxidationsstabilität mit beschleunigtem Oxidationsverfahren und kleiner Probenmenge (RSSOT), DIN EN 16091:2022-12., https://dx.doi.org/10.31030/3360235
7. Spectrometers for Elemental Spectrochemical Analysis, Part IV: Inductively Coupled Plasma Optical Emission Spectrometers, Spectroscopy-09-01-2011, volume 26, Issue 9, https://www.spectroscopyonline.com/view/spectrometers-elemental-spectrochemical-analysis part-iv-inductively-coupled-plasma-optical-emission?utm_source=chatgpt.com
8. J.H. van ‘t Hoff, Studies in Dynamic Chemistry, 1884

8 Acknowledgement

The author(s) would like to thank the partners in the project for their valuable comments on previous drafts and for performing the review.

Project partners:

#	Partner short name	Partner Full Name
1	CSIC	AGENCIA ESTATAL CONSEJO SUPERIOR DE INVESTIGACIONES CIENTIFICAS
2	MPG	MAX-PLANCK-GESELLSCHAFT ZUR FORDERUNG DER WISSENSCHAFTEN EV
3	DTU	DANMARKS TEKNISKE UNIVERSITET
4	OWI	OWI SCIENCE FOR FUELS GMBH
5	UNR	UNIRESEARCH BV
6	T4F	TEC4FUELS GmbH
7	AVL	AVL LIST GMBH
9	UZ	SVEUCILISTE U ZAGREBU. FAKULTET STROJARSTVA I BRODOGRADNJE
10	UCT	UNIVERSITY OF CAPE TOWN
11	KAUST	KING ABDULLAH UNIVERSITY OF SCIENCE AND TECHNOLOGY

This project has received funding from the European Union's Horizon Europe research and innovation programme under grant agreement No 101083700. Views and opinions expressed are however those of the author(s) only and do not necessarily reflect those of the European Union. Neither the European Union nor the granting authority can be held responsible for them.